Hyperfine Interactions manuscript No.
(will be inserted by the editor)

T.M. Mendonça · A.M.L. Lopes · J.N. Gonçalves · J.G. Correia · P.B. Tavares · V.S. Amaral · C. Darie · J.P. Araujo

Perturbed Angular Correlations Investigations on $YMnO_3$ Multiferroic Manganite

Received: date / Accepted: date

Abstract The Perturbed Angular Correlation (PAC) technique was applied to study the yttrium local environment in $YMnO_3$ multiferroic manganite. The electric field gradients (EFG) at the Y site have been measured as function of temperature, covering both ferroelectric and magnetic transitions. The results were compared with point charge model (PCM) calculations.

The experimental results show two different EFG distributions for all temperatures. Only one can be directly attributed to the yttrium crystalline site in the hexagonal structure.

Keywords PAC · manganites · Phase separation

1 Introduction

The rare-earth manganites system, $RMnO_3$, present a rich variety of interesting properties such as colossal magneto-resistance [1] or magneto-electric effect [2,3]. These properties are known to be closely related to the crystalline structure, which depends on the rare-earth ionic radius. The decrease of the rare-earth ionic radius (R_I) induces a change in the crystalline structure from an orthorhombic (for larger R, R=La-Dy) to hexagonal (for smaller R, R=Ho-Lu and Y) structure. Moreover, the magneto-electric coupling has also different origins depending on the crystalline structure: in the orthorhombic $RMnO_3$, ferroelectricity appears coupled to the magnetic ordered phase [2] while in the hexagonal $RMnO_3$ ferroelectric ordering is due to the unusual rare-earth sites coordination and the triangular and layered MnO_5 network [4]. The hexagonal manganites structure consists of non-connected layers of MnO_5 trigonal bipyramids corner-linked by in-plane oxygen atoms forming close-packed planes separated by a layer of R^{3+} ions. At high temperatures, these compounds undergo a phase transition from a high-symmetry phase (space group $P6_3/mmc$), which is paraelectric, to a low temperature non centrosymmetric phase (space group $P6_3cm$) that is spontaneously polarized [4].

T.M. Mendonça · J.P. Araujo
IFIMUP and IN - Institute of Nanosciences and Nanotechnologies, Porto, Portugal
Tel.: +351-22-0402362
Fax: +351-22-0402406
E-mail: taniamel@mail.cern.ch

A.M.L. Lopes · J.G. Correia
Centro de Fisica Nuclear da Universidade de Lisboa, Lisboa, Portugal

J.N. Gonçalves · V.S. Amaral
Departamento de Fisica and CICECO, Universidade de Aveiro, Aveiro, Portugal

P.B. Tavares
CQVR - Departamento de Quimica, Univ. Tras-os-Montes e Alto Douro, Vila Real, Portugal

T.M. Mendonca · C. Darie
Institut Neel, CNRS, Grenoble, France

The properties of these compounds depend strongly on the rare-earth coordination and local environment. In this context, nuclear hyperfine techniques can be particularly useful to study the local lattice structure, electric and magnetic correlations. With this aim in view, the perturbed angular correlation (PAC) technique has been used to determine the electric field gradients (EFG) that depends on local charge distributions at the probe atom site in $YMnO_3$ as function of temperature, covering both magnetic and ferroelectric transitions.

2 Experimental

Polycrystalline samples of $YMnO_3$ were synthesized via a sol-gel route using urea as complexing agent. The resulting powders were subjected to several thermal treatments and sintered at 1623 K, in air for 72 hours, followed by quenching to room temperature. The quality of the samples has been controlled using X-ray diffraction (XRD) and magnetic measurements. The lattice parameters refinements based on XRD data were performed using the program Full Prof Suite [5].

The PAC experiments have been performed by first implanting the samples with ^{111m}Cd ($T_{1/2}$=49 min) to a low dose of 1.0×10^{12} at/cm^2 and 30 keV energy at the ISOLDE/CERN facility [6]. After implantation, the samples were annealed at 973K in air, for 20 min to remove implantation damage [7]. The ^{111m}Cd isotope decays to the I=5/2 and E=245 keV isomeric state of ^{111}Cd with the emission of two consecutive γ-rays. The angular correlation between the two γ-rays is perturbed by the EFG and the magnetic hyperfine field (MHF), which is described by the experimental time perturbation function, R(t), which were obtained using a 6-BaF_2 detector spectrometer [8]. The measurements have been performed at 10 K, room temperature and 1123K, across the ferroelectric and magnetic transitions. The fits to the R(t) experimental functions were calculated numerically by taking into account the full Hamiltonian for the nuclear quadrupole/magnetic combined interactions [9]. The experimental results were compared with point charge model (PCM) calculations where the EFG is calculated by taking the ion cores as point charges located at the ions lattice sites. Different atoms were differentiated by the Sternheimer antishielding factor γ_∞ [10–12].

3 Results and Discussion

The refinement of X-ray data show that $YMnO_3$ samples are single phase and crystallize in the hexagonal structure (space group $P6_3cm$) with corresponding cell parameters a=b=6.1354(1) Å and c=11.3916(3) Å in excellent agreement with the values reported in the literature [13,14]. Since the XRD measurements have been performed at room temperature, the obtained structure is the non-centrosymmetric, which allows the appearance of ferroelectricity. Magnetic measurements show a paramagnetic-antiferromagnetic transition at $T_N\sim75$ K, also in good agreement with the values reported in literature [13,14].

Fig. 1(a) shows representative experimental function R(t) (left panel) and respective Fourier transforms (right panel), for measurements performed at 1123 K, room temperature and 10 K. The high quality fits are shown by continuous lines in the R(t) spectra. The fit to each experimental spectrum was obtained considering that the ^{111}Cd probes interact with two electric field gradient (EFG) distributions for all temperatures, which were assumed to be Lorentzian-like. Fig. 1(b) displays the thermal dependence of the EFG parameters (fraction of probes interacting with each EFG (f), principal component of the EFG tensor (V_{zz}) and asymmetry parameter (η)).

The R(t) spectra show essentially the same features for all temperatures. As referred above, the best fit to each R(t) spectrum revealed that the ^{111}Cd probes interact with two EFG (named EFG_a and EFG_b) distributions. The main EFG, EFG_a, is characterized by a lower V_{zz} and is non-axially symmetric with $\eta_a\sim0.2(8)$. The second EFG, EFG_b, is characterized by a higher V_{zz} and a highly asymmetric local environment given by η values ranging between 0.5-0.6. The Fourier transforms show a decrease on the main peak intensity with temperature. A close inspection to the plot obtained at 10 K, below the magnetic ordering, suggest the existence of a weak magnetic hyperfine field (MHF). Thus, a combined interaction (quadrupolar and magnetic) was used in EFG_a distribution accounting for a weak MHF ($B_{Hf}\sim0.1(2)$ T).

As one can observe in Fig. 1(b), the EFG parameters show a weak dependence on the measuring temperature. The fraction of probes interacting with each EFG, f_a and f_b, is constant with temperature.

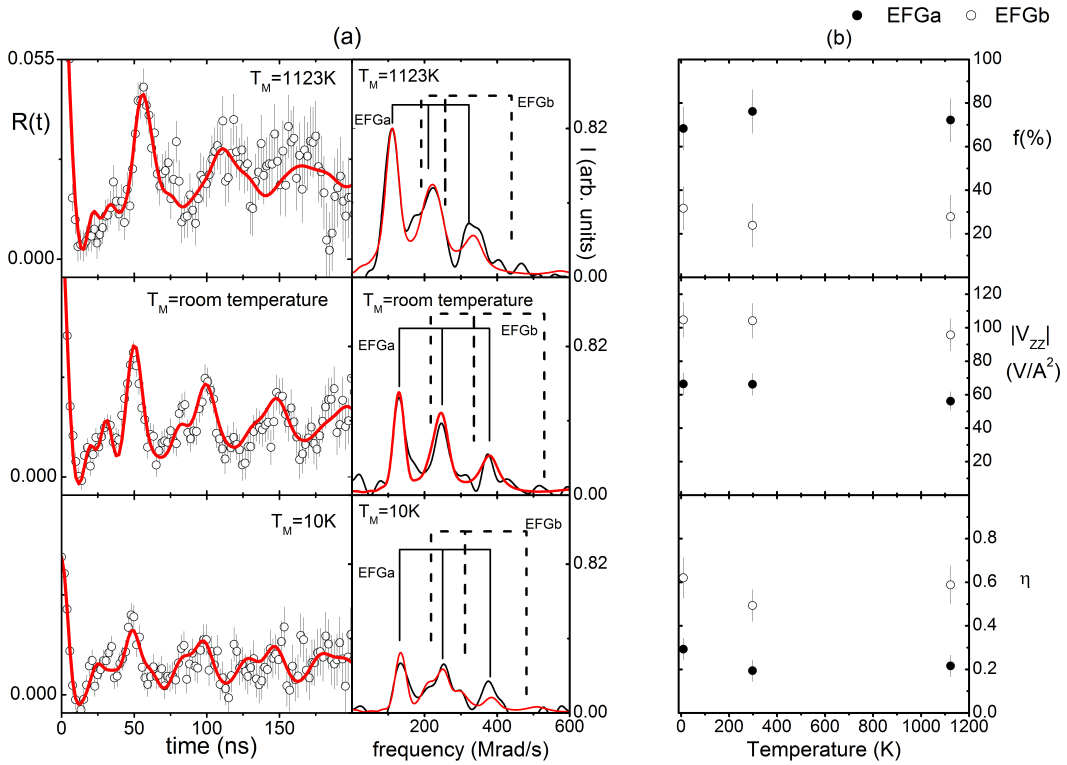

Fig. 1 (a) Left panel: Representative R(t) experimental functions measured at 1123K, room temperature and 10K. Right panel: respective Fourier transforms. The vertical solid and dashed lines indicate the frequency triplets corresponding to each EFG. (b)Electrical field gradient parameters, fraction of probes (f), V_{ZZ} and η as function of temperature.

The EFG principal component, V_{zz}, shows the typical decrease on its magnitude with increasing temperature for both EFG_a and EFG_b. This trend was found in perovskite systems [15,16] and is frequently associated to an increase of the atomic vibrations due to the increase of temperature. The asymmetry parameter, η, is also constant with temperature, with small variations within the error bars for both EFG distributions.

The existence of two experimental EFG distributions would tempt the direct assignment to the rare-earth crystallographic sites allowed by the $P6_3cm$ space group (R(2a site) and R(4b site)). On the other hand, at 1123K, $YMnO_3$ is in the paraelectric phase (T_{FE}~1050K [17]) and adopts the centrosymmetric space group $P6_3/mmc$, which allows only one non-equivalent Y site and therefore the existence of only one possible EFG. Hence the origin of EFG_b cannot be directly assigned to the regular yttrium site. To help in the interpretation of the present PAC experimental results, point charge model calculations (PCM) have been performed, which were later confirmed by full potential linearized augmented plane wave (FLAPW) calculations [18]. The lattice parameters, for the different space groups, were taken from literature [14,19] and the formal charges of +3, +3 and -2 were assigned to Y, Mn and oxygen atoms respectively. The lattice sum was performed up to a distance of 25 Å from the probe nucleus. Table 1 shows the resulting values of the calculated V_{zz} and η in comparison with the experimental ones. When comparing these calculated values with the experimental ones, one can observe that only one of the experimental EFG distributions is in good agreement with the calculated ones. Following these results, EFG_a can be directly assigned to the Y2 (4a site) although the experimental asymmetry parameter is higher than the calculated (η=0). This discrepancy may be due to the polycrystalline nature of this ceramic sample. The second EFG_b experimental distribution cannot be assigned either to Y1 or Mn sites, which calculated EFG parameters are very different from the experimental ones. Also, the very weak MHF measured at 10K suggests that the ^{111}Cd probe atoms are not located at the Mn site, where a higher MHF would be expected. Based on XRD and magnetic measurements, also performed after the PAC experiments, the high quality of the samples show that

Table 1 Experimental and calculated EFG parameters in the yttrium and manganese sites with substitutional Cd. The calculated EFG parameters were obtained for high temperature (space group $P6_3/mmc$) and low temperature (space group $P6_3cm$) structures. V_{zz} values are in V/Å^2.

Experimental EFG				Calculated EFG									
				S.G.$P6_3/mmc$				S.G.$P6_3cm$					
V_{zza}	η_a	V_{zzb}	η_b	V_{zz} (Y)	η (Y)	V_{zz} (Mn)	η (Mn)	V_{zz} (Y_1)	η (Y_1)	V_{zz} (Y_2)	η (Y_2)	V_{zz} (Mn)	η (Mn)
2.18	0.2(8)	3.44	0.5(1)	2.25	0	-7.30	0.13	0.45	0	2.18	0	-7.89	0.06

the origin of this EFG_b also cannot be attributed to impurities. Thus the origin of the higher V_{zzb} local environment is not clear and do not seem related to the quality of the samples nor defects created by the implantation process since previous studies showed that the present annealing was sufficient to recover from implantation defects [15,16]. The existence of this second EFG distribution seems to be intrinsic to this system and has to be found in more subtle grounds.

4 Conclusions

The EFG evolutions as a function of temperature in the $YMnO_3$ manganite has been studied via the PAC technique. The PAC experimental results show two different EFG distributions for all temperature ranges. However, only one experimental EFG can be directly attributed to the Y crystalline site in the hexagonal structure. The origin of the second local environment is still unclear and seems to be intrinsic to the system. Additional studies are needed to unveil these results.

Acknowledgements This work was supported by the Portuguese Foundation for Science and Technology, FCT, with the projects CERN-FP-83643-2008, CERN-FP-83506-2008, CERN-FP-109272-2009, CERN-FP-109357-2009, PTDC/FIS/105416/2008, by the EU (FP6 RII3-EURONS, Contract N. 506065), by the German BMBF funding resources and by the ISOLDE Collaboration with approved project IS487. T.M. Mendonça acknowledges FCT PhD grant SFRH/BD/29445/2006.

References

1. Dagotto, E.: Complexity in strongly correlated electronic systems. Science **309**, 257 (2005)
2. Kimura, T., et al.: Magnetic control of ferroelectric polarization. Nature **426**, 55 (2003)
3. Fiebig, M., et al.: Observation of couples magnetic and electric domains. Nature **419**, 818 (2002)
4. Van Aken, B.B., et al.: The origin of ferroelectricity in magnetoelectric $YMnO_3$. Nature Mater. **3**, 164 (2004)
5. Rodriguez-Carvajal, J.: Recent advances in magnetic structure determination by neutron powder diffraction. Physica B **192**, 55 (1993)
6. Kugler, E., et al.: The new CERN-ISOLDE on-line mass-separator facility at the PS-Booster. Nucl. Instrum. Methods Phys. Res. B **70**, 41 (1992)
7. Araujo, J.P., et al.: Electrical field gradient studies on $La_{1-x}Cd_xMnO_{3+\delta}$ system. Hyperfine Inter. **158**, 347 (2004)
8. Butz T., et al.: A 'TDPAC-Camera'. Nucl. Instrum, Methods Phys. Res. B **47**, 417 (1989)
9. Barradas, N.P., et al.: Magnetic anisotropy and temperature dependence of the hyperfine fields of single-crystalline cobalt. Phys. Rev. B **47**, 8763 (1993)
10. Schmidt, P.C., et al.: Effect of self-consistency and crystalline potential in the solid state on nuclear quadrupole Sternheimer antishielding factors in closed-shell ions. Phys. Rev. B **22**, 4167 (1980)
11. Gupta, R.P., et al.: Sternheimer shielding-antishielding.II. Phys. Rev. A **8**, 1169 (1973)
12. Feiock, F.D., et al.: Atomic susceptibilities and shielding factors. Phys. Rev. **187**, 39 (1969)
13. Lee, S., et al.: Giant magneto-elastic coupling in multiferroic hexagonal manganites. Nature **451**, 805 (2008)
14. Van Aken, B.B., et al.: Hexagonal $YMnO_3$. Acta Crystall. C **57**, 230 (2001)
15. Lopes, A.M.L., et al.: Percolative transition on ferromagnetic insulator manganites: uncorrelated to correlated polaron clusters. Phys. Rev. B **73**, 100408(R) (2006)
16. Lopes, A.M.L., et al.: New phase transition in the $Pr_{1-x}Ca_xMnO_3$ system: evidence for electrical polarization in charge ordered manganites. Phys. Rev. Lett. **100**, 155702 (2008)
17. Lonkai, Th., et al.: Development of high-temperature phase of hexagonal manganites. Phys. Rev. B **69**, 134108 (2004)
18. Mendonça, T.M., et al.: To be published
19. Jeong, I.-K., et al.: High-temperature structural evolution of hexagonal multiferroic $YMnO_3$ and $YbMnO_3$. J. Appl. Cryst. **40**, 730 (2007)